J. Mol. Biol. (1997) 271, 656–668

JMB

Consideration of the pH-dependent Inhibition of Dihydrofolate Reductase by Methotrexate

William R. Cannon*, Barbara J. Garrison and Stephen J. Benkovic*

Department of Chemistry
152 Davey Laboratory
Pennsylvania State University
University Park
PA 16802, USA

Poisson-Boltzmann calculations were used to determine the pK_a of protein functional groups in the unliganded dihydrofolate reductase enzyme, and the pK_a of protein and ligand groups in methotrexate-enzyme complexes. The results reported here are in conflict with two fundamental tenets of dihydrofolate reductase inhibition by methotrexate: (1) Asp27 is not expected to be protonated near pH 6.5 in the apoenzyme as previously proposed based on fitting of empirical equations to binding data, and (2) the calculated pK_a for the pteridine N1 of the inhibitor while bound to the protein is significantly lower than that estimated for this group from interpretation of NMR data (>10). In fact, the electrostatic calculations and complementary quantum chemical calculations indicate that Asp27 is likely protonated when methotrexate is bound, resulting in a neutral dipole-dipole interaction rather than a salt-bridge between the enzyme and the inhibitor. Reasons for this discrepancy with the experimental data are discussed. Furthermore, His45 and Glu17 in the *Escherichia coli* enzyme are proposed to be in part responsible for the pH dependence of the conformational degeneracy in the inhibitor-enzyme complex.

*Corresponding authors

Keywords: dihydrofolate reductase; methotrexate; inhibition; pH; pK_a

Introduction

Methotrexate (MTX) is a small molecule inhibitor of the ubiquitous enzyme dihydrofolate reductase (DHFR), which is a requisite component of the biosynthetic pathway for purine and pyrimidine synthesis. As a consequence, MTX is used as a drug for the treatment of a wide range of diseases including many cancers, infections, rheumatoid arthritis, multiple sclerosis and lupus. Its success as a therapeutic agent is due in large part to its strong binding to DHFR. Despite the structural similarity of MTX to the DHFR substrate dihydrofolate (H_2F), as shown in Figure 1, MTX binds to DHFR three or more orders of magnitude more strongly than folate substrates such as H_2F (Stone & Morrison, 1983b, 1986). As such, MTX serves not only as a potent therapeutic agent that can be administered in relatively small amounts, but it also serves as an important model for molecular recognition in host-guest chemistry.

A major difference between the binding of the substrate H_2F and MTX is the strongly pH-dependent nature of MTX binding. This titration behavior has been characterized by pH-dependent binding studies (Stone & Morrison, 1983b), nuclear magnetic resonance spectroscopy (Cocco *et al.*, 1981, 1983; London *et al.*, 1986) and examination of the rates of MTX binding and release by the enzyme (Appleman *et al.*, 1988). Although titration phenomena are known to be important in binding of MTX to DHFR and in general for molecular recognition, the complexity of interactions among the many titratable groups in biological molecules and their complexes with ligands makes the molecular interpretation of data difficult.

For example, in order to evaluate the role that titratable groups on both the inhibitor and the enzyme play in binding, empirical equations are often used in fitting the experimental data obtained from pH-dependent binding studies in order to obtain pK_a values (Cleland, 1977; Stone & Morrison, 1983a). As such, the interpretation of the experimental data is constrained by the set of equations employed in obtaining the fit, which are derived from simple binding equations and generally allow for only several titratable groups.

DHFR from *Escherichia coli*, however, contains 159 amino acid residues, approximately one-third of which contain side-chains which undergo acid-base titrations. Although it is apparent from struc-

Abbreviations used: MTX, methotrexate; DHFR, dihydrofolate reductase; PABA, para-aminobenzoic acid.

0022–2836/97/340656–13 $25.00/0/mb971173

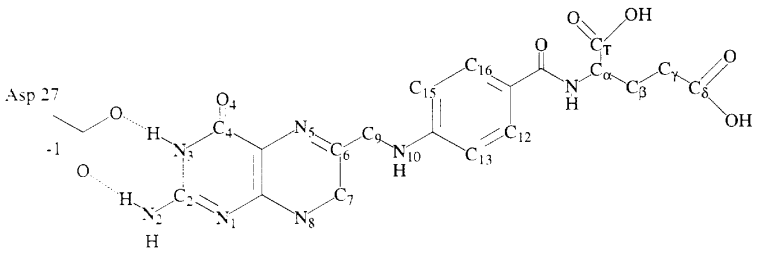

A. H_2F

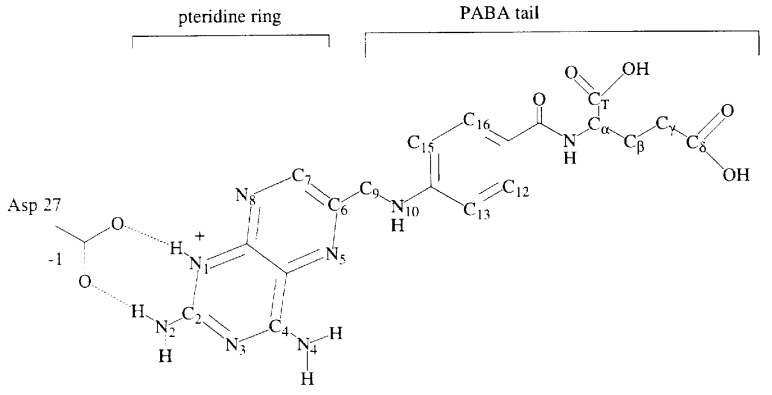

B. MTX

Figure 1. A, Structure of the substrate, dihydrofolate, and B, the tight-binding inhibitor, methotrexate.

tural studies on DHFR that only a few of these groups directly interact with bound inhibitors or substrates (Bolin *et al.*, 1982), long-range electrostatic interactions of groups removed from the binding site must be accounted for along with those groups which titrate upon the conformational changes induced by binding. Both DHFR inhibition and catalysis are known to be pH-dependent, however the nature of the pH-dependence has been a subject of debate for some time (Fierke *et al.*, 1987; Cocco *et al.*, 1981; Cayley *et al.*, 1981; Stone & Morrison, 1983b; Chen *et al.*, 1994).

As a result of early binding studies, it was concluded that Asp27 was protonated in the free enzyme, characterized by a pK_a of 6.6 (Stone & Morrison, 1983b), and this proposal has since served as a basic tenet of the mechanics of DHFR inhibition and catalysis (Brown & Kraut, 1992). The electrostatic nature of the enzyme active site has further been examined by nuclear magnetic resonance studies (Cocco *et al.*, 1981, 1983; London *et al.*, 1986), in which the bound MTX inhibitor is apparently protonated at the pteridine N1 even at pH 10, despite the fact that in solution the pK_a of this site on the inhibitor is only 5.7. The partial structure of the binding site is shown in Figure 2. In the *E. coli* enzyme, MTX binds with its pteridine ring rotated by 180° with respect to the conformation of the pterin ring of bound H_2F (Figure 1; Bolin *et al.*, 1982), thus allowing the interaction of the pteridine N1 with the only ionizable residue in the active site of the enzyme, Asp27 (Figures 1B and 2). Despite the proposed protonation of Asp27 in the unbound enzyme, binding of the inhibitor is thought to result in the formation of a salt-bridge between an ionized Asp27 and the protonated form of the inhibitor. Presumably, the large difference in proton affinity

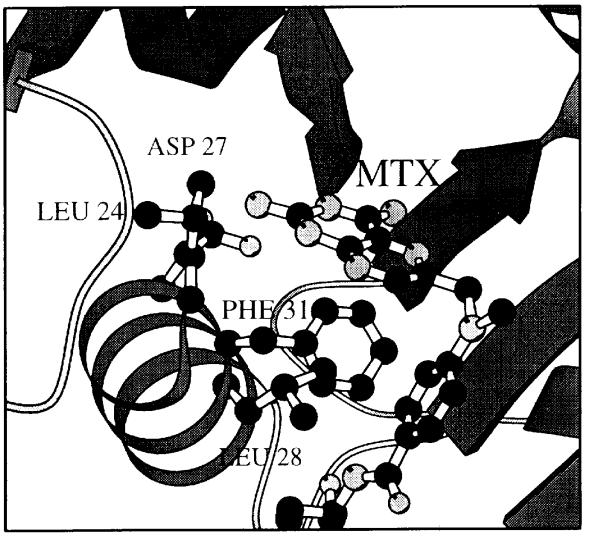

Figure 2. View of the binding site of DHFR with MTX and the hydrophobic active site residues Leu24, Asp27, Leu28 and Phe31 shown (Asp27 is partially hidden behind Leu24). Graphics made with the MOLSCRIPT software (Kraulis, 1991).

between the bound and unbound states of the inhibitor is due to the formation of this salt-bridge. Such a strong perturbation of the proton affinity/energetics of a bound ligand would be important, as polarization of substrates by enzymes is often proposed as a mechanism of catalysis. Furthermore, the strong binding of MTX to DHFR relative to the substrate H_2F is thought to be related to the ability of MTX to form this salt-bridge with the enzyme, however this explanation has been questioned due to results from free energy simulations (Singh & Benkovic, 1988).

Here, we report the results of Poisson-Boltzmann calculations on the apoenzyme and two methotrexate-enzyme crystallographic structures. These calculations were used to characterize the titration behavior of the MTX inhibitor-enzyme complex relative to the apoenzyme, which has no bound ligands. Two conformations of the enzyme-inhibitor complex were examined that differ with respect to the solvent accessibility to the active site and in the interactions of two titratable residues. For both the apoenzyme and the enzyme-inhibitor complex the results are reported as a change in the pK_a of the group on the enzyme relative to the same group in solution. The results indicate that Asp27 in the apoenzyme is ionized near physiological pH, and that the binding of MTX to DHFR involves a neutral dipole-dipole interaction rather than a salt-bridge as determined by NMR studies. The latter result is shown to be consistent with quantum chemical models of the Asp27-MTX interaction. Possible explanations for this apparent discrepancy with NMR chemical shift data are discussed. Additionally, the electrostatic calculations also implicate a pair of titratable residues, Glu17 and His45, as being important in the conformational degeneracy of the enzyme-inhibitor complex. The utility of the Poisson-Boltzmann analysis in prediction of molecular properties is evident from the results of a recent Raman difference study on DHFR which was published while this manuscript was being revised. In agreement with the work presented here and our previous study (Cannon *et al.*, 1997) it was found that Asp27 is not protonated in the apoenzyme (Chen *et al.*, 1997).

Methods

Proton affinities

Calculation of pK_as was done using the method of Antosiewicz *et al.*, 1994). The pK_as for amino acid groups in solution, as determined by experiment, were used as model pK_as and the starting points of the calculations. The linearized Poisson-Boltzmann equation was then used to determine pK_a values for the same groups in the enzyme environment. The enzyme was modeled as a low-dielectric medium characterized by a dielectic constant (ε) of 20 and comprises point charges representing the partial charges of atoms. The extent of the enzyme enviroment was determined by the Richards solvent accessible surface (Richards, 1977). The solvent was modeled as a high-dielectric medium ($\varepsilon = 80$) having an ionic strength of 150 mM. Poisson-Boltzmann electrostatic calculations were carried out using the UHBD program (Davis *et al.*, 1991), employing dielectric smoothing (Davis & McCammon, 1991; Gilson *et al.*, 1993) at the enzyme-water dieletric boundary, and finite difference focusing techniques (Gilson *et al.*, 1988). The "intrinsic" proton affinities (pK_a^{int}), which do not include contributions from ionized states of residues, are determined from:

$$pK_a^{int} = pK_a^{model} - z[\Delta\Delta G/2.303RT]$$

where z is 1 for a base and -1 for an acid, R is the gas constant, T is the temperature, and $\Delta\Delta G$ is the ionization free energy difference for transfer of the model residue in solution to the site in the neutral enzyme. A temperature of 298 K was used in all calculations. The final pK_a value was determined by allowing interactions between ionizable residues in their charged states and determining the lowest energy ionization state of the structure using the method of clustering ionizable groups (Gilson, 1993).

Stability curves

The determination of pK_as for the apoenzyme allows a comparison of the calculated pH dependence of unfolding to that determined experimentally. The free energy of unfolding is related to the average net protonic charge of the folded and unfolded states through the relation (Yang & Honig, 1993; Antosiewicz *et al.*, 1994):

$$\frac{\partial(\Delta G)}{\partial \mathrm{pH}} = 2.303RT(\langle q_{\mathrm{unfolded}}\rangle - \langle q_{\mathrm{folded}}\rangle) \qquad (1)$$

The average net protonic charge of the unfolded state is determined by assuming the groups in the unfolded protein titrate according to the pK_a of individual amino acids free in solution (pK_a^{model}). As the apoenzyme is missing Glu17 in the crystallographic structure, the pH-dependent stability as determined by the calculations assumes that this residue titrates at the same pK_a in the crystallographic structure as in the unfolded state. Furthermore, the calculations only take into account electrostatic energies and neglect contributions to the unfolding free energy from sources such as the hydrophobic effect. As such, regardless of the accuracy of the calculations, the calculated results will differ from the true value by a constant.

Computational details

For amino acids the model dissociation acid constants, pK_a^{model}, are the dissociation constant values for each amino acid side-chain in solution (Stryer, 1981; Nozaki & Tanford, 1967). Model values for MTX are the pK_as of the titratable sites on MTX in

Table 1. Model and calculated pK_as ($\varepsilon = 20$) for MTX

	N1	N5	C_δ	C_ζ
Model (Poe, 1973, 1977)	5.7	−1.5	4.7	3.4
MTX-B	6.1	−6.8	4.7	0.5
MTX-A	6.1	−7.2	4.5	0.1

solution as determined by experiment (Poe, 1973, 1977) and are listed in Table 1.

Structures for the apo-enzyme and the DHFR·MTX binary complexes were obtained from the Protein Data Bank, files 5dfr (Bystroff & Kraut, 1991) and 4dfr (Bolin *et al.*, 1982), respectively. Polar hydrogen atoms were added using the CHARMm molecular modeling package (Molecular Simulations Inc., San Diego, CA), except for aspartic acid, glutamic acid and histidine residues, which were added manually. The crystallographic structure for the apo protein (5dfr) is missing residues 16 to 20 because of disorder in the crystal structure, and therefore these are not accounted for in the electrostatic calculations. The unit cell for the DHFR·MTX structure contains two unique structures, refered to as MTX-A and MTX-B. The latter structure is more complete and thus recommended for use in the Protein Data Bank file. However, because the two structures contain differing configurations of groups undergoing ionization, both structures were utilized in the study.

The potential parameters used here were the same as those used in the original method (Antosiewicz *et al.*, 1994), with the exception of MTX partial charges. CHARMm partial charges along with OPLS Lennard-Jones parameters were used for all amino acid residues. Lennard-Jones parameters for the para-aminobenzoic acid moiety of MTX were adopted from the analogous OPLS parameters for benzene (Jorgensen & Severance, 1990), and the carboxylic acid and amide moieties (Jorgensen & Tirado-Rives, 1988). The pteridine ring Lennard-Jones parameters were adopted from similar OPLS atom types for nucleotide bases (Pranata & Jorgensen, 1991). Partial charges for the MTX inhibitor were determined from quantum chemical Hartree-Fock calculations using the *Gaussian 92* program (Frisch *et al.*, 1992) and the 3-21G basis set. The electrostatic field from the quantum chemical calculation was fit to a point charge model by a least-squares optimization using the CHELPG algorithm (Breneman & Wiberg, 1990), and are given in the Appendix, Table A1. (Use of these parameters for molecular mechanics simulations would require further development. Although the charges obtained in this manner provide a good representation of the surrounding electrostatic field, the charges, atomic radii and dispersion energies must be matched appropriately for use in molecular mechanics simulations.)

Ionization of the MTX acid groups were modeled in a manner analogous to that for amino acid side-chains: a full charge of −1 was placed on the corresponding carboxylate carbon. Protonation of the MTX base sites was modeled as placement of an additional charge of +1 on the corresponding heavy atom, the pteridine N1 or N5.

Quantum chemical potential energy surfaces

A model potential energy surface for the transfer of a proton from a neutral Asp27 to MTX, resulting in a slat-bridge, was determined by employing a 4-aminopteridine ring as a model for MTX and acetic acid as a model for the carboxylic acid group of Asp27. The configuration of the acetic acid-pteridine ring was taken from the crystallographic structure of the enzyme-inhibitor complex (Bolin *et al.*, 1982) and geometry optimized *in vacuo*. The theoretical model employed the hybrid functional method of Becke (1993) with a split valence basis set, b3lyp/6-31G(d)> The optimization resulted in a distance of 2.77 Å between N1 of the pteridine ring and the closest acetic acid oxygen; the same distance found in the crystallographic structures is 2.5 to 2.6 Å. The actual distance employed in the potential energy surface scan was 2.75 Å.

The potential energy surface for the proton transfer occurring *in vacuo* ($\rho = 1$) and that for a surrounding dielectric continuum with $\varepsilon = 4$ and $\varepsilon = 10$ were determined. The proton was initially placed on the acetate oxygen at a distance of 0.95 Å and then incrementally moved onto the pteridine N1. The distance between the acetate oxygen and the pteridine N1 was held fixed (2.75 Å) while all other degrees of freedom were allowed to relax. The dielectric environment was modeled by the Onsager reaction field method (Wong *et al.*, 1991) and the *Gaussian 92* program was used for these calculations (Frisch *et al.*, 1992).

Results

Overview

The results are discussed in the context of the calculated pK_a, which takes into account desolvation and interactions with other charges in the protein, and the intrinsic pK_a which is simply the pK_a of the residue when only desolvation and dipole-dipole interactions are taken into account in an otherwise neutral protein. That is, the intrinsic pK_a does not include the effect of charge-charge interactions due to titrations of other groups. Desolvation of a molecule or group involves the crossing of a boundary which distinguishes the high-dielectric solvent from the low-dielectric protein interior, and has been shown to cost up to 20 to 50 kcal mol^{-1} in model protein systems (Gilson *et al.*, 1985; Gilson & Honig, 1988). The intrinsic pK_a is a convenient way to separate the effects of desolvation from those due to the influence of other charge groups, particularly as the effect of desolvation and charge-charge interactions can counteract each other leading to negligible changes with respect to the group in solution, or the effects may be com-

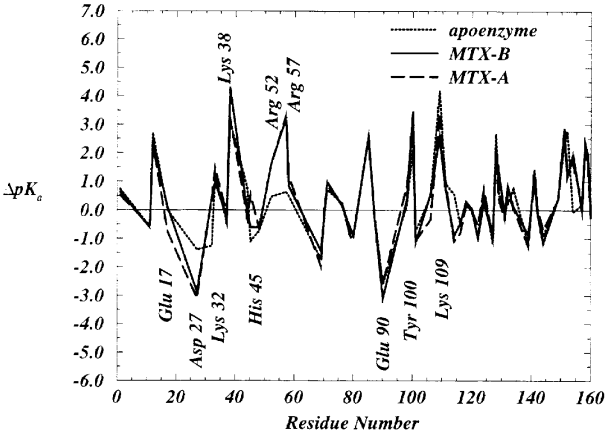

Figure 3. Shifts in pK_a between model solution values and values calculated for the protein environment for residues of the apoenzyme and residues of the two enzyme-inhibitor complexes.

pounded so as to result in large shifts from the solution pK_a.

Figure 3 compares the titration behavior of the two DHFR·MTX binary complexes and the apoenzyme, in which the pK_a shift (ΔpK_a) between the calculated pK_a of the residue in the protein and the pK_a of the same group in solution (pK_a^{model}) is plotted against the residue number. (The pK_as of all protein residues are given in the Appendix, Table A2.) The apoenzyme has several residues which exhibit titration behavior different from that seen in the MTX-bound structures, and not surprisingly most of these residues are involved in binding MTX. These residues are discussed first†. Next, we will compare results for the two enzyme-inhibitor complexes obtained from the protein data base, MTX-A and MTX-B, which exhibit similar titration behavior with only a few exceptions. Finally, the results for the apoenzyme can be compared to data from pH-dependent stability studies (Jennings, 1991). The general implications of this work for the pH-dependent inhibition of DHFR by MTX and the strong binding of MTX relative to the substrate H_2F will be discussed in the last section.

Comparison of apoenzyme with enzyme-inhibitor complexes

Binding the pteridine ring: classical results

In the apoenzyme structure, the results from the Poisson-Boltzmann analysis indicate that the catalytically important residue Asp27 is shifted below its solution value of 4.0. Loop 1 is missing in the apoenzyme structure, however, and may partially desolvate the pocket in which Asp27 is located, increasing the pK_a of this residue relative to the value determined here. Nevertheless, the effect of the loop is likely to be minimal, as the fact that the loop is disordered in the crystal structure indicates that it is highly mobile and is not likely to decrease the local dielectric response significantly. This supposition is supported by the results obtained for the enzyme-cofactor structure (Cannon *et al.*, 1997) in which loop 1 is ordered and a similar pK_a is found.

The titration behavior of Asp27 is significantly affected by binding of MTX, as is N1 of the pteridine ring of MTX. Since Asp27 is important for catalysis, and the salt-bridge between Asp27 and N1 of MTX has been implicated in the strong binding of MTX by DHFR, we examined the titration behavior of these residues by determining their pK_as as a function of the dielectric constant used for the protein interior. Although the actual dielectric response of the protein interior varies as a function of position in the protein, from a low of about 4 in the interior to higher values on the protein surface where residues have more conformational freedom, a value of 20 has been shown to result in a good statistical fit to experimentally determined pK_as. In this regard it has been shown that using a dielectric constant of 4 for the protein interior and directly examining different protein conformational states leads to improved results over pK_a values obtained when using a dielectric of 4 and a static structure (You & Bashford, 1995). Enzyme and substrate groups located in the active site, however, are not as likely to have significant conformational freedom due to the need to provide a stable environment for the catalytic reaction (Cannon *et al.*, 1996). Furthermore, the pK_a of such a buried group may be underestimated by employing dielectric constant of 20 for the protein interior (Antosiewicz *et al.*, 1994). In this case, the use of a lower dielectric constant may be most appropriate (Demchuk & Wade, 1996).

The results obtained at different values of the dielectric constant (ε) are shown in Figure 4, in which both the pK_a (thick line) and the intrinsic pK_a (thin line) are shown for each group. In the apoenzyme the carboxylate form of Asp27 is desta-

† There are two trivial differences between the apoenzyme structure and the MTX-bound structures which affect the results. First, as the crystal structure for the apoenzyme is missing loop 1 (residues 16 to 20), the calculated pK_a shift for Glu17 appears as 0.0. For the enzyme-inhibitor structure MTX-B the pK_a of Glu17 is unaffected by transfer into the protein environment ($\Delta pK_a = 0.1$), but in the MTX-A structure the same residue is shifted down from its solution value by 0.8.

Second, the difference in pK_as for His114 in the MTX-bound structures relative to the apoenzyme is a result of the difference in primary sequences of the DHFR enzymes. The DHFR enzyme used in the MTX·DHFR crystallographic study differs from the apoenzyme and other structures of *E. coli* DHFR by having a lysine residue at position 154 rather than a glutamic acid. His114 is involved in a salt-bridge with residue 154, and as a result the MTX·DHFR structures have a different pK_a for this residue. The calculated pK_a for Glu154 is 4.3 in the apoenzyme. The pK_a for Lys154 in the MTX-A structure is 12.0 while that for the MTX-B structure is 12.3.

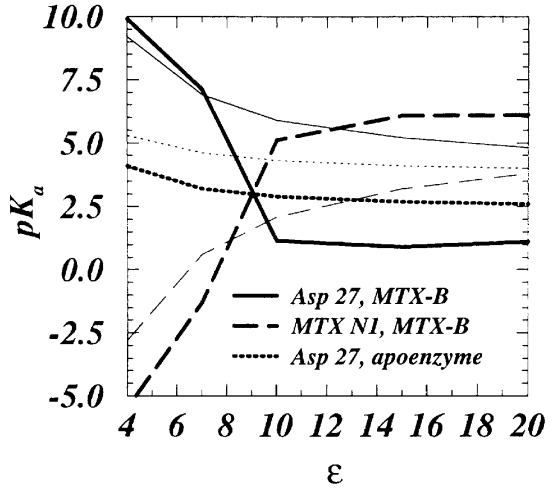

Figure 4. Intrinsic pK_a (thin lines) and final calculated pK_a (thick lines) of the active site residue Asp27 (apoenzyme and MTX-B structures) and N1 of the inhibitor MTX (MTX-B structure) as a function of the protein dielectric constant, ε.

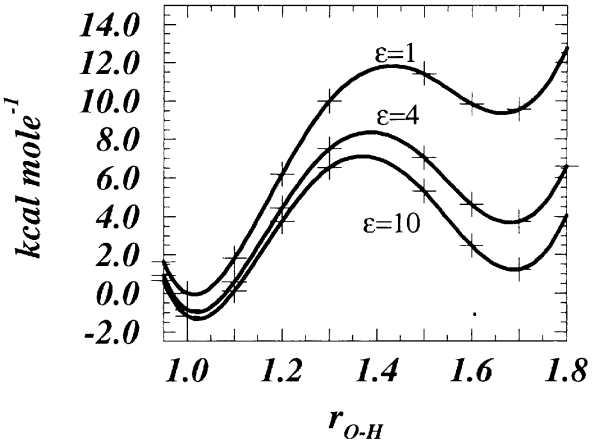

Figure 5. Potential energy surface for the transfer of a proton from acetic acid to N1 of the pteridine ring of MTX in various dielectric environments (ε). Small values of $r_{O\text{-}H}$ correspond to the acetic acid/pteridine pair and larger values correspond to the acetate/pteridinium pair.

bilized as the dielectric constant of the protein decreases, as indicated by the increase in pK_a as the dielectric constant decreases from 20 to 4. However, even with a dielectric constant of 4, the pK_a of Asp27 is only 4.1 in the apoenzyme.

The intrinsic pK_a of Asp27 in both of the MTX·DHFR complexes is shifted upwards from the solution value for all values used for the dielectric constant of the protein interior, due to the greater work required to ionize the carboxyl group in the low-dielectric active site when MTX is bound, and due to the unfavorable dipolar interaction of this residue with the unprotonated N1 of the pteridine ring of MTX as indicated in Figure 1B. Identical titration behavior is seen in the MTX-A structure of the inhibitor-enzyme complex (data not shown). Effects from charge-charge interactions can compensate somewhat for the influence of desolvation, especially those due to protonation of the pteridine N1, however the net result is not enough to form a salt-bridge between the pteridine N1 and Asp27 when a dielectric constant of less than 10 is used.

A dielectric constant greater than 10 acts to lower the relative energy of the Asp27-MTX salt-bridge to such an extent that the proton transfers from the carboxylic acid side-chain of Asp27 to N1 of MTX and this then becomes the low-energy state. However, even then the estimated pK_a is not shifted significantly higher than that observed for MTX in solution (6.1 *versus* 5.7, respectively). Because of this issue, we further examined the titration behavior of the binary DHFR·MTX structure using a similar method which takes into account the full charge distribution of the ionized state of the titratable group (Antosiewicz *et al.*, 1996a). The results were in agreement with those presented here, except that the salt-bridge was unstable throughout the protein dielectric range of 4 to 20 (data not shown). Since NMR chemical shift data implies that this salt-bridge is maintained even above pH 10, we further examined the potential energy surface using quantum chemical techniques.

Binding the pteridine ring: quantum chemical results

The potential energy surfaces for the transfer of a proton from acetic acid to a 4-aminopteridine ring using different dielectric environments is shown in Figure 5. The orientation for these groups are essentially the same as that observed crystallographically for Asp27-MTX. The energy surface *in vacuo* ($\varepsilon = 1$) strongly favors the protonation of the acetate to form acetic acid; a local minimum for protonation of N1 of the pteridine ring exists 8.5 kcal $mole^{-1}$ above the ground state minimum. When a dielectric constant of 4 is used to characterize the environment, this local minimum is reduced to within 4.5 kcal $mole^{-1}$ of the ground state; however, the ground state is still the neutral acetic acid-pteridine pair. Increasing the dielectric constant to 10 further reduces the energy of the ion pair relative to the neutral species; however, the reduction is still not enough to make the ion pair the favored conformation. Although more sophisticated techniques could be used to model the reaction field or environment of the acetic acid-pteridine pair, this model is expected to give results which are within the accuracy required for this problem (Foresman *et al.*, 1996).

Groups involved in binding the PABA moiety of MTX

Lys32, Arg52 and Arg57 are involved in binding the two carboxylate groups of the PABA tail of

MTX, and as a consequence the pK_as of these groups are shifted upward relative to the apoenzyme. These three residues form an ionic cluster on the surface of the protein with the two carboxylate groups of the PABA tail of MTX, and they have previously been implicated by electrostatic calculations as significant for substrate binding (Bajorath *et al.*, 191). Titration results for the groups of the MTX PABA tail are shown in Table 1. The intrinsic pK_a of each carboxylic acid is essentially unchanged from the solution pK_a; however one of these groups (C_T) is sandwiched between Lys32 and Arg57, resulting in a downwards shift in pK_a due to charge-charge interactions.

Tyr100, which interacts with the enzyme cofactor during catalysis, is also somewhat perturbed in the MTX structures relative to the apoenzyme. Although similar shifts are seen in the holoenzyme and ternary complex (Cannon *et al.*, 1997), this perturbation is not due to binding of the enzyme cofactor, NADPH. Instead, binding of MTX results in exclusion of water molecules in the active site and a decrease in the local dielectric constant, but not to the extent seen in structures containing NADPH (Cannon *et al.*, 1997. As a result, the intrinsic pK_a of this group is shifted upwards somewhat in the MTX structure. Furthermore, the decrease in the local dielectric response allows nearby charged residues to have a greater influence on ionization of Tyr100, as seen in the calculations on the holoenzyme (Cannon *et al.*, 1997). In this regard, it is likely that Asp27, which is ionized at physiological pH, further increases the pK_a of Tyr100.

A surface cluster of titratable residues

Lys38 and Lys109 are central structural components of a cluster of ionizable residues that involve diverse secondary structural domains. As an element of the eight-strand β-sheet A, Lys109 is in contact with Glu90, a loop residue between helices 4 and 5, and Glu157 which is part of strand 2 of β-sheet A. Additionally, Lys109, Glu90 and Lys38 form a salt-bridge triad on the surface of the enzyme. Lys38 lies just beyond the C terminus of helix 2 and may be important for aligning helix 2, the N terminus of which contains the catalytically important Asp27. This cluster is located on the backside of the enzyme with respect to the active site, and the interdomain nature of these charge-charge interactions suggest that they may be involved in proper folding of the enzyme or perhaps creating an architecture conducive to catalysis.

The pK_as of Lys38 and Lys109 are differentially shifted in the MTX-A, MTX-B and apoenzyme structures. The causes of these shifts are unknown, but they are also observed in structures of the holoenzyme and ternary enzyme complex with substrate (Cannon *et al.*, 1997). The differential shifts for Lys109 must be due to interactions with other titratable groups and not due to desolvation, as the intrinsic pK_a for Lys109 in the apoenzyme is 10.5, that for the MTX-B structure is 10.2, and that for the MTX-A structure is 10.4, while the final pK_as after charge-charge interactions are accounted for are 14.6, 12.9 and 13.8, respectively. Likewise, the intrinsic pK_as for Lys38 in the same structures are 10.5, 10.7 and 10.4, while the final values are 13.5, 14.7 and 13.7. The increased pK_a for Lys109 in the apoenzyme with respect to either MTX-bound structure suggests that there is a stronger electronegative field in the vicinity of Lys109 in the apoenzyme; however, the identification of the source of such a field may be difficult due to the complex nature of the ionic clustering.

Comparison of enzyme-inhibitor complexes

The two DHFR·MTX structures differ in titration behavior primarily at two residues, Glu17 and His45. This can be anticipated from the crystallographically determined structures, as the major structural difference between MTX-A and MTX-B is the location of loop 1, which contains Glu17 (Bolin *et al.*, 1982), as shown in Figure 6. In the MTX-A structure, the side-chains of Glu17 and His45 are 3.4 Å apart and as such it can be expected that the proton affinity of each residue is affected by the charge due to the other residue. This is borne out in the calculations. Although the intrinsic pK_a for Glu17 in the MTX-A structure is 4.6 and that for His45 is 5.7, charge-charge interactions shift the pK_as downward to 3.6 for Glu17 and upwards to 6.8 for His45.

In the MTX-B structure, the residues are no longer in close proximity. The intrinsic pK_a for Glu17 is then 4.3 while that for His45 is 5.5. Inclusion of ionization states in the calculation has little further effect, as the final pK_a for Glu17 is 4.5, while that for His45 is 5.7.

Discussion: Comparison with Experiment

Unfolding of the apoenzyme

The Poisson-Boltzmann calculations allow a comparison of the calculated pH dependence of unfolding to that determined experimentally. The results are shown in Figure 7, in which the calculated stability curve has been visually overlaid on the experimental data (Jennings, 1991). Qualitatively, the agreement between calculation and experiment is reasonably good. The shape of the stability curve is reproduced between pH 6.3 and 9.5, for which experimental data are available. The calculated stability reaches a maximum at pH 5, below which it decreases rapidly. Previous work has shown that the stability curves generated by this method result in a good overall shape of the curve when compared with experiment, but that the pH dependence of the curve tends to be too steep due to the sensitive dependence of the shape of the curve on equation (1) (Antosiewicz *et al.*, 194). That is, as most groups tend to titrate at the same pH in the folded state as in the unfolded

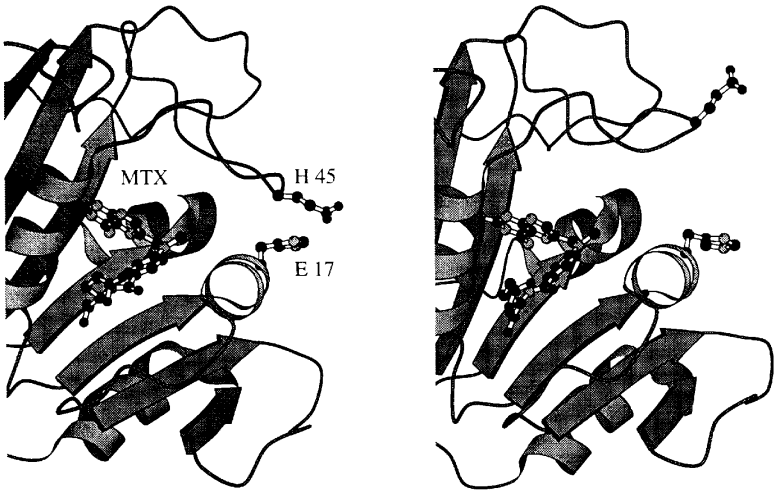

Figure 6. Comparison of the two crystallographic structures of MTX-bound DHFR in which the active site lid, loop 1 (residues 9 to 24), is either closed or open. Graphics made with the MOLSCRIPT software (Kraulis, 1991).

state, the shape of the titration curve is dependent on the few groups with significantly shifted pK_as. Thus, a small error in a calculated pK_a can change the slope of the stability curve noticeably. Another source of disagreement between calculated and experimental stability curves, however, is the assumption that the crystallographic structure is an adequate representative of the ensemble of structures that constitute the thermodynamic folded state. In this regard, it is also likely that at the extremes of pH for which the crystallographic structure is marginally stable, the protein conformation adjusts to other substates and with differing pK_as in order to minimize the change in free energy with respect to pH. This buffering effect would mitigate steep changes in stability with respect to pH.

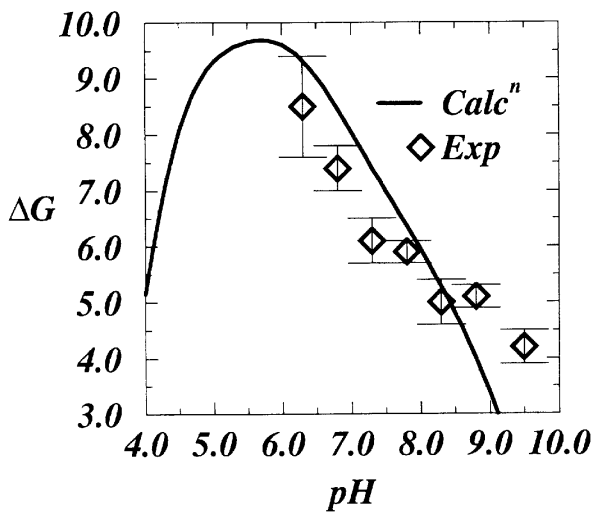

Figure 7. Comparison of the pH dependence of protein stability as determined from experiment and the Poisson-Boltzmann calculations.

Inhibitor binding: salt-bridge or neutral polar interaction?

The results for Asp27 and N1 of the MTX pteridine ring presented here differ significantly from values found in the literature. Both nuclear magnetic resonance studies (Cocco *et al.*, 1981, 1983; London *et al.*, 1986) and pH-dependent competitive binding studies (Stone & Morrison, 1983b) indicate that bound MTX remains protonated at least to pH 10, in disagreement with the calculated pK_a range reported here of 6.1 (protein dielectric of 20) to approximately 1 (protein dielectric of 4). Because a dielectric in the range of 4 to 10 is probably more appropriate for the buried groups of Asp27 and the pteridine ring of MTX in the binary structure, the calculations indicate that the interaction between Asp27 and MTX is a neutral dipole-neutral dipole interaction rather than a salt-bridge. As such, the results from the Poisson-Boltzmann calculation are in qualitative as well as quantitative disagreement with the interpretation of NMR chemical shifts.

This represents a significant puzzle. The calculated pK_as are quite reasonable within the framework of classical electrostatics. Desolvation of the pteridine ring during binding acts to decrease rather than increase the observed pK_a due to the desire to bury the pteridine ring as a neutral species rather than a charged one in the low dielectric environment of the active site. As shown in Figure 2, the intrinsic pK_a of N1 of bound MTX is shifted below the solution value of 5.7 for all values of the protein dielectric constant examined. Only with a relatively high value for the dielectric constant of the protein interior ($\varepsilon = 20$) is the pK_a shifted back upward towards a value (6.1) close to that found for MTX in solution (5.7). Below a dielectric constant of 10, however, the salt-bridge is unstable and it is the neutral species which exist. These results are also in agreement with free-

energy simulations in which it was concluded that the contribution of the salt-bridge to the binding energy is insignificant, as the enzyme environment does not stabilize the salt-bridge enough to pay the energetic cost of desolvating the charge groups (Singh & Benkovic, 1988).

In contrast, desolvation and burial of Asp27 upon MTX binding to the enzyme should significantly increase the pK_a of this group due to (1) the greater work required to ionize this residue in the lower dielectric environment and (2) the favorable dipolar interaction formed between the carboxylic acid residue O-H and the pteridine N1. Unlike the energetics of the salt-bridge configuration, the combined effects of desolvation and charge-charge interactions with other protein groups are favorable to a large upwards shift in pK_a, as demonstrated in Figure 4.

Since the electrostatic calculations only addressed pK_a shifts due to classical electrostatic effects, quantum chemical calculations with a simple model for the surrounding environment were used to examine the potential energy surface for transfer of the proton from the carboxyl oxygen to N1 of the pteridine ring of methotrexate, as shown in Figure 5. For all dielectric environments examined, the proton is preferentially located on the aspartic acid group, rather than on the pteridine ring which would result in a salt-bridge.

One might be tempted to believe that the effective dielectric constant of the active site of the enzyme is still quite high since in the DHFR·MTX structures there are several crystallographically observable water molecules. However, even when the cofactor NADPH binds to DHFR and displaces these water molecules, thereby ensuring a low-dielectric environment, the NMR study indicates that the salt-bridge does not collapse (London *et al.*, 1986). Furthermore, the distance between the carboxyl oxygen and the pteridine N1 appears to decrease from 2.6 to 3.0 Å in the structures of the binary DHFR·MTX complex (4dfr, Bolin *et al.*, 1982; 1dds, 1ddr, Yennawar & Farber, 1995) to 2.3 to 2.6 Å in the ternary DHFR·NADPH·MTX structures (3dfr, Bolin *et al.*, 1982; 1rx3 Sawaya & Kraut, 1997; the resolutions of these structures range from 1.7 to 2.2 Å, however. The NMR data, however, indicate that there is no change in the protonation state of MTX between the binary and ternary complexes. Even more perplexing is that NMR chemical shifts of the ternary DHFR·NADPH·MTX complex are nearly identical with those of the ternary DHFR·$NADP^+$·MTX complex (Cheung *et al.*, 1992). The oxidized and positively charged nicotinamide ring is nearly stacked on top of the pteridine ring of MTX which is also assumed to be protonated because of the chemical shift data, yet the nicotinamide ring atoms are most likely greater than 7.5 Å from the carboxylic acid group of Asp27, so that the orientation of charges in the low-dieletric active site is comparable to $++-$ rather than $+-+$. $NADP^+$ is not capable of losing its charge by proton titration, and it is surprising to find that both MTX and $NADP^+$ have buried positive charges in close proximity.

At this point we are unable to explain this descrepancy between theory and experiment. There are, however, several possibilities. First, the charge model used for MTX is not from a standardized parameter set, but is derived from quantum chemical calculations. Different partial charges, however, do not appear likely to change the qualitative nature of the MTX titration observed in the calculations when using a protein dielectric of 20 (Antosiewicz *et al.*, 1996b). The use of a lower protein dielectric combined with a different charge set will likely produce quantitatively different results, but it is unlikely that those results will be qualitatively different from those reported here.

It may be that the solution and crystal structures of the DHFR·MTX complex are significantly different. Formation of the Asp27-MTX salt-bridge within the framework of classical electrostatics would require a stabilizing electrostatic field, which might be provided by the cobinding of an ion from solution. Binding of a cation in the active site of acetylcholine esterase appears to be responsible for a pK_a shift that is observed experimentally but not in electrostatic calculations (Wlodek *et al.*, 1995). DHFR is known to be inhibited by ions (Poe *et al.*, 1972; Erickson & Mathews, 1973; Baccanari *et al.*, 1975), and the buffer used in the NMR studies contained 100 mM potassium phosphate. However, given that the pK_a of MTX appears to be shifted even when MTX and the cofactor $NADP^+$ are bound, this phenomenon seems less likely in this case. Instead, the decrease in activity observed experimentally with high salt concentration may be due to stabilization of the charge on Asp27 by an increased ionic strength.

Yet another possibility is that classical electrostatic theory alone is not sufficient to describe the shift in pK_a of MTX between the enzymic and solution environments, and that a more sophisticated electrostatic field is required to model the protein environment in the quantum mechanical calculations. However, previous calculations of pK_as for protein groups which utilized the Poisson-Boltzmann equation have resulted in root-mean-square deviations with experiment of only 0.9 pH units (Antosiewicz *et al.*, 1994). Anomolous results due to unaccounted for quantum chemical effects have not been reported. It has been noted in other combined quantum chemical/continuum electrostatic solvation studies that the continuum reaction field does not adequately account for the relative change in solvation energy across the series NH_3, NH_2CH_3, $NH(CH_3)_2$, $N(CH_3)_3$ (Marten *et al.*, 1996). However, in that case the relevant interaction between solute and solvent was not explicitly accounted for with quantum mechanical models, while in the present case the relevant interaction between the pteridine ring of MTX and the carboxylic acid moeity of Asp27 is explicitly modeled quantum mechanically.

The influence of nearby aromatic groups may also be important (M. K. Gilson & M. Krauss, personal communication) however, as they have been shown to stabilize cation binding (Dougherty, 1996). In the active site of DHFR the side-chain of Phe30 lies over the MTX pterin ring in crystal structures, and likewise, the benzoyl ring of MTX folds back towards the pterin ring in a manner which may help to stabilize a salt-bridge (Figure 2). These groups are not accounted for in the quantum chemical calculations, and a point charge model for these aromatic rings may not be adequate to observe such effects in the electrostatic calculations. If this is the case, influence of these groups may also be important in catalysis: protonation of the substrate dihydrofolate must occur at the pterin N5, either by transfer from the pterin O4 (Cannon *et al.*, 1997), or direct protonation of N5 (Chen *et al.*, 1994).

The close distance found between the Asp carboxyl oxygen and N1 of the MTX pteridine ring observed in the structure of the ternary complex of DHFR·MTX·NADPH (2.3 Å), may also provide an important clue. Such a small distance between heavy atoms is often associated with a single potential energy minimum for the proton between the two heavy atoms (Scheiner & Kar, 1995). Although the proton is not expected to be equally shared between the oxygen and nitrogen, such a configuration may provide an explanation for the conflicting qualitative behavior of the pK_a shift and the observed NMR chemical shift. The classical electrostatic approach assumes a double minimum for the proton exists between the two heavy atoms. Likewise, the quantum chemical calculations only examined an intermolecular separation (2.75 Å) in which a double minimum exists. Potential energy surfaces are presently being examined for short intermolecular separations that would result in a single potential energy minimum for the proton, as are the corresponding chemical shifts of these configurations. If this is indeed the case, the distinction between a neutral polar interaction and a salt-bridge may not be clear. Previous determinations of such potential energy surfaces have indicated that the relative energies of the salt-bridged and neutral polar atomic configurations do not change depending on whether a single or double minimum exists (Scheiner & Kar, 1995); however, it is not clear what effect there would be on the chemical shift data.

Conformational dependence on pH

The titration behavior of the two DHFR·MTX crystal structures differs primarily at Glu17 and His45, implying that these residues play an important role in the pH dependence of MTX binding. Although the two enzyme-inhibitor structures MTX-A and MTX-B may have configurational artifacts due to crystal-packing forces, pH dependence of the equilibrium between two DHFR·MTX conformers has been observed experimentally by NMR (Huang *et al.*, 1991). Similarly, NMR studies of the apoenzyme have also demonstrated that the E_1, E_2 isomers also differ by the conformation of loop 1 (Falzone *et al.*, 1994), which contains Glu17. In analogy with the DHFR·MTX complex then, it can be anticipated that His45 is also involved in the conformational equilibria of the apoenzyme. Studies by Dunn *et al.* (1990) have demonstrated that the equilibrium between the E_1, E_2 isomers of the apoenzyme are pH dependent with a pK_a of 5.2 for the E_2 conformer and 6.0 for the E_1 conformer. The former value is similar to the pK_a of 5.2 found for His45 in the apoenzyme here. Furthermore, NADPH binds to just one of the apoenzyme conformers and binding is at a maximum at pH 6.0. If the apoenzyme conformers are indeed analogous to the enzyme-inhibitor conformers, then the apoenzyme in which the active site gate, loop 1, is in an open position will be the conformer which is required in order to bind to NADPH.

Conclusion

The ability of the electrostatic calculations to readily access the trends in the titration behavior of individual residues suggests that in the apoenzyme the pK_a of Asp27 is near 3, and that the pK_a of the pteridine ring of MTX is not dramatically shifted higher in the enzyme environment relative to the solution value. Both electrostatic and quantum chemical calculations find that protonation of Asp27 to form a neutral polar interaction with the inhibitor is more favorable than formation of an enzyme-inhibitor salt-bridge. The NMR chemical shift data, however, appear to convincingly establish the existence of a salt-bridge between the inhibitor and the enzyme. The discrepancy between theory and experiment may be due to a single potential energy minimum for the proton between the heavy atoms of the enzyme and the inhibitor, or to the influence of nearby aromatic groups. This proposal and the data presented here warrant further investigation of the interaction between the enzyme and inhibitor.

Acknowledgments

We are indebted to J. A. McCammon for providing the UHBD program, J. Antosiewicz for providing programs and files necessary for carrying out the titration calculations, and M. K. Gilson, J. M. Briggs and B. Honig for helpful suggestions. This work was supported by grants NIH GM24129 (S. J. B.) and NSF CHE-9317429 (B. J. G.). W. R. C. is a NIH postdoctoral fellow.

References

Antosiewicz, J., McCammon, J. A. & Gilson, M. K. (1994). Prediction of pH-dependent properties of proteins. *J. Mol. Biol.* **238**, 415–436.

Antosiewicz, J., Briggs, J. M., Elcock, A. H., Gilson, M. K. & McCammon, J. A. (1996a). Computing ionization states of proteins with a detailed charge model. *J. Comput. Chem.* **17**, 1633–1644.

Antosiewicz, J., McCammon, J. A. & Gilson, M. K. (1996b). The determinants of pK_as in proteins. *Biochemistry*, **35**, 7819–7833.

Appleman, J. R., Howell, E. E., Kraut, J., Kühl, M. & Blakely, R. L. (1988). Role of Asp27 in the binding of methotrexate to dihydrofolate reductase from *Escherichia coli*. *J. Biol. Chem.* **263**, 9187–9198.

Baccanari, D., Phillips, A., Smith, S., Sinski, D. & Burchall, J. (1975). Purification and properties of *Escherichia coli* dihydrofolate reductase. *Biochemistry*, **14**, 5267–5273.

Bajorath, J., Li, Z., Fitzgerald, G., Kitson, D. H., Farnum, M., Fine, R. M., Kraut, J. & Hagler, A. T. (1991). Changes in the electron density of the cofactor NADPH on binding to *E. coli* dihydrofolate reductase. *Proteins: Struct. Funct. Genet.* **11**, 263–270.

Becke, A. D. (1993). Density-functional thermochemistry. III. The role of exact exchange. *J. Chem. Phys.* **98**, 5648–5652.

Bolin, J. T., Filman, D. J., Matthews, D. A., Hamlin, R. C. & Kraut, J. (1982). Crystal structures of *Escherichia coli* and *Lactobacillus casei* dihydrofolate reductase refined at 1.7 Ångstroms resolution. I. General features and binding of methotrexate. *J. Biol. Chem.* **257**, 13650–13662.

Breneman, C. & Wiberg, K. (1990). Determining atom-centered monopoles from molecular electrostatic potentials: the need for high sampling density in formamide conformational analysis. *J. Comput. Chem.* **11**, 361–373.

Brown, K. A. & Kraut, J. (1992). Exploring the molecular mechanism of dihydrofolate reductase. *Faraday Discuss.* **93**, 217–224.

Bystroff, C. & Kraut, J. (1991). Crystal structure of unliganded *Escherichia coli* dihydrofolate reductase. Ligand-induced conformational changes and cooperativity in binding. *Biochemistry*, **30**, 2227–2239.

Cannon, W. R., Singleton, S. F. & Benkovic, S. J. (1996). A perspective on biological catalysis. *Nature Struct. Biol.* **3**, 821–833.

Cannon, W. R., Garrison, B. J. & Benkovic, S. J. (1997). Electrostatic characterization of enzyme complexes: reevaluation of the mechanism of catalysis of dihydrofolate reductase. *J. Am. Chem. Soc.* **119**, 2386–2395.

Cayley, P. J., Dunn, M. J. & King, R. W. (1981). Kinetics of substrate, coenzyme, and inhibitor binding to *Escherichia coli* dihydrofolate reductase. *Biochemistry*, **20**, 874–879.

Chen, Y. Q., Kraut, J., Blakely, R. L. & Callender, R. (1994). Determination by Raman spectroscopy of the pK_a of N5 of dihydrofolate reductase: mechanistic implications. *Biochemistry*, **33**, 7021–7026.

Chen, Y. Q., Kraut, J. & Callender, R. (1997). pH-dependent conformational changes in *Escherichia coli* dihydrofolate reductase revealed by Raman difference spectroscopy. *Biophys. J.* **72**, 936–941.

Cheung, H. T. A., Birdsall, B. & Feeney, J. (192). ^{13}C NMR studies of complexes of *Escherichia coli* dihydrofolate reductase formed with methotrexate and with folic acid. *FEBS Letters*, **312**, 147–151.

Cleland, W. W. (1977). Determining the chemical mechanisms f enzyme-catalyzed reactions by kinetic studies. *Advan. Enzymol. Relat. Areas Mol. Biol.* **45**, 273–389.

Cocco, L., Groff, J. P., Temple, C., Jr, Montgomery, J. A., London, R. E., Matwiyoff, N. A. & Blakely, R. L. (1981). Carbon-13 nuclear magnetic resonance study of protonation of methotrexate and aminopterin bound to dihydrofolate reductase. *Biochemistry*, **20**, 3972–3978.

Cocco, L., Roth, B., Temple, C., Jr, Montgomery, J. A., London, R. E. & Blakely, R. L. (1983). Protonated state of methotrexate, trimethoprim, and pyrimthamine bound to dihydrofolate reductase. *Arch. Biochem. Biophys.* **226**, 567–577.

Davis, M. E. & McCammon, J. A. (191). Dielectric boundary smoothing in finite difference solutions of the Poisson equation: an approach to improve accuracy and convergence. *J. Comput. Chem.* **12**, 909–912.

Davis, M. E., Madura, J. D., Luty, B. A. & McCammon, J. A. (1991). Electrostatics and diffusion of molecules in solution: simulations with the University of Houston Brownian dynamics programs. *Comput. Phys. Commun.* **62**, 187–197.

Demchuk, E. & Wade, R. C. (1996). Improving the continuum dielectric approach to calculating pK_a of ionizable groups in proteins. *J. Phys. Chem.* **100**, 17373–17387.

Dougherty, D. A. (1996). Cation-pi interactions in chemistry and biology: a new view of benzene, Phe, Tyr, and Trp. *Science*, **271**, 163–168.

Dunn, S. M., Lanigan, T. M. & Howell, E. E. (1990). Dihydrofolate reductase from *Escherichia coli*: probing the role of aspartate-27 and phenylalanine-137 in enzyme conformation and the binding of NADPH. *Biochemistry*, **29**, 8569–8576.

Erickson, J. S. & Mathews, C. K. (1973). Dihydrofolate reductases of *Escherichia coli* and bacteriophage T4. A spectrofluorometric study. *Biochemistry*, **12**, 372–380.

Falzone, C. J., Wright, P. E. & Benkovic, S. J. (1994). Dynamics of a flexible loop in dihydrofolate reductase from *Escherichia coli* and its implication for catalysis. *Biochemistry*, **33**, 439–442.

Fierke, C. A., Johnson, K. A. & Benkovic, S. J. (1987). Construction and evaluation of the kinetic scheme associated with dihydrofolate reductase. *Biochemistry*, **26**, 4085–4092.

Foresman, J. B., Keith, T. A., Wiberg, K. B., Snoonian, J. & Frisch, M. J. (1996). Solvent effects. 5. Influence of cavity shape, truncation of electrostatics, and electron correlations on ab initio reaction field calculations. *J. Phys. Chem.* **100**, 16098–16104.

Frisch, M., Head-Gordon, M., Trucks, G., Foresman, J., Schlegel, H., Raghavachari, K., Robb, M., Binkley, J., Gonzalez, C., Defrees, D., Fox, D., Whiteside, R., Seeger, R., Melius, C., Baker, J., Martin, R., Kahn, L., Stewart, J., Topiol, S. & Pople, J. (1992). *Gaussian 92*. Gaussian, Inc., Pittsburgh, PA.

Gilson, M. K. (193). Multiple-site titration and molecular modelling: two rapid methods for computing energies and forces for ionizable groups in proteins. *Proteins: Struct. Funct. Genet.* **15**, 266–282.

Gilson, M. K. & Honig, B. H. (198). Calculation of the total electrostatic energy of a macromolecular system: solvation energies, binding energies, and conformational analysis. *Proteins: Struct. Funct. Genet.* **4**, 7–18.

Gilson, M. K., Rashin, A., Fine, R. & Honig, B. (1985). On the calculation of electrostatic interactions in proteins. *J. Mol. Biol.* **183**, 503–516.

Gilson, M. K., Sharp, K. A. & Honig, B. H. (1988). Calculating the electrostatic potential of molecules in solution: method and error assessment. *J. Comput. Chem.* **9**, 327–335.

Gilson, M. K., Davis, M. E., Luty, B. A. & McCammon, J. A. (1993). Computation of electrostatic forces on solvated molecules using the Poisson-Boltzmann equation. *J. Phys. Chem.* **97**, 3591–3600.

Huang, F. Y., Yang, Q. X. & Huang, T. H. (1991). 15N NMR studies of the conformation of *E. coli* dihydrofolate reductase in complex with folate or methotrexate. *FEBS Letters*, **289**, 231–234.

Jennings, P. A. (1991). Biophysical studies of the mechanism of folding of dihydrofolate reductase from *Escherichia coli*. Ph.D. thesis, Pennsylvania State , University, University Park, PA.

Jorgensen, W. L. & Severance, D. L. (1990). Aromatic-aromatic interactions: free energy profiles for the benzene dimer in water, chloroform, and liquid benzene. *J. Am. Chem. Soc.* **112**, 4768–4774.

Jorgensen, W. J. & Tirado-Rives, J. (1988). The OPLS potential functions for protein. Energy minimizations for crystals of cyclic peptides and crambin. *J. Am. Chem. Soc.* **110**, 1657–1666.

Kraulis, P. J. (1991). MOLSCRIPT: a program to produce both detailed and schematic plots of protein structures. *J. Appl. Crystallog.* **24**, 946–950.

London, R. E., Howell, E. E., Warren, M. S., Kraut, J. & Blakely, R. L. (1986). Nuclear magnetic resonance study of the state of protonation of inhibitors bound to mutant dihydrofolate reductase lacking the active-site carboxyl. *Biochemistry*, **25**, 7229–7235.

Marten, B., Kim, K., Cortis, C., Friesner, R. A., Murphy, R. B., Ringnalda, M. N., Sitkoff, D. & Honig, B. (1996). New model for calculation of solvation free energies: correction of self-consistent reaction field continuum dielectric theory for short-range hydrogen-bonding effects. *J. Phys. Chem.* **100**, 11775–11788.

Nozaki, Y. & Tanford, C. (1967). Examination of titration behavior. *Methods Enzymol.* **11**, 715–734.

Poe, M. (1973). Proton magnetic resonance studies of folate, dihydrofolate, and methotrexate. *J. Biol. Chem.* **248**, 7025–7032.

Poe, M. (1977). Acidic dissociation constants of folic acid, dihydrofolic acid, and methotrexate. *J. Biol. Chem.* **252**, 3724–3728.

Poe, M., Greenfield, N. J., Hirshfield, J. M., Williams, M. N. & Hoogsteen, K. (1972). Dihydrofolate reductase. Purification and characterization of the enzyme from an amethopterin-resistant mutant of *Escherichia coli*. *Biochemistry*, **11**, 1023–1030.

Pranata, J. & Jorgensen, W. L. (1991). OPLS potential functions for nucleotide bases. Relative association constants of hydrogen bonded base pairs in chloroform. *J. Am. Chem. Soc.* **113**, 2810–2819.

Richards, F. M. (1977). Areas, volumes, packing and protein structures. *Annu. Rev. Biophys. Bioeng.* **6**, 151–176.

Sawaya, M. R. & Kraut, J. (1997). Loop and subdomain movements in the mechanism of *Escherichia coli* dihydrofolate reductase: crystallographic evidence. *Biochemistry*, **36**, 586–603.

Scheiner, S. & Kar, T. (1995). Nonexistence of specially stabilized hydrogen bonds in enzymes. *J. Am. Chem. Soc.* **117**, 6970–6976.

Singh, U. C. & Benkovic, S. J. (1988). Probing the salt-bridge in the dihydrofolate reductase-methotrexate complex by using the coordinate-coupled free-energy perturbation method. *Proc. Natl Acad. Sci. USA*, **85**, 4280–4284.

Stone, S. R. & Morrison, J. F. (1983a). The interaction of an ionizing ligand with enzymes having a single ionizing group. *Biochim. Biophys. Acta*, **745**, 237–246.

Stone, S. R. & Morrison, J. F. (1983b). The pH-dependence of the binding of dihydrofolate and substrate analogues to dihydrofolate reductase from *Escherichia coli*. *Biochim. Biophys. Acta*, **745**, 247–258.

Stone, S. R. & Morrison, J. F. (1986). Mechanism of inhibition of dihydrofoalte reductases from bacterial and vertebrate sources by various classes of folate analogues. *Biochim. Biophys. Acta*, **869**, 275–285.

Stryer, L. (1981). *Biochemistry*, 2nd edit., W. H. Freeman and Co., New York.

Wlodek, S. J., Antosiewicz, J., McCammon, J. A. & Gilson, M. K. (1995). *Modelling of Biomolecular Structures and Mechanisms*, Kluwer Academic, Dordrecht, Boston.

Wong, M. W., Frisch, M. J. & Wiberg, K. B. (1991). Solvent effects. 1. The mediation of electrostatic effects by solvents. *J. A,. Chem. Soc.* **113**, 4776–4782.

Yang, A. S. & Honig, B. (1993). On the pH dependence of protein stability. *J. Mol. Biol.* **231**, 459–474.

Yennawar, H. P. & Farber, G. K. (1995). Protein Data Base entries 1dds and 1ddr.

You, T. J. & Bashford, D. (1995). Conformation and hydrogen ion titration of proteins: a continuum electrostatic model with conformational flexibility. *Biophys. J.* **69**, 1721–1733.

Appendix

Table A1. Charges from quantum chemical calculations and actual charges employed in the electrostatic calculations

Atom	HF/3-21G	Chg used
N1	−0.975562	−0.980
C2	1.179473	1.180
N2	−1.095492	−1.100
H2a	0.458863	0.460
H2b	0.443826	0.440
N3	−0.886996	−0.890
C4	0.740291	0.740
N4	−0.865573	−0.870
H4a	0.416445	0.420
H4b	0.376295	0.380
C4a	−0.156023	−0.160
N5	−0.478367	−0.480
C6	0.309537	0.300
C7	0.194539	0.190
H7	0.100182	0.100
N8	−0.634634	−0.630
C8a	0.896238	0.900

For a comparison of HF/3-21G and HF/6-31G* charges for pterin systems, see Cannon *et al.* (1997).

Table A2. pK_a values for protein residues of the apoenzyme and the two MTX-bound enzymes

Group	Model	Calculated pK_a			Group	Model	Calculated pK_a		
		Apo	MTX-B	MTX-A			Apo	MTX-B	MTX-A
MetN1	7.5	8.2	8.1	8.0	Lys106	10.4	10.8	10.9	10.0[a]
Asp11	4.0	3.4	3.4	3.4	Lys109	10.4	14.5	12.8	13.7
Arg12	12.0	14.6	14.3	14.2	Tyr111	9.6	10.5	10.3	10.5
Glu17	4.4	0.0[a]	4.5	3.6	HisB114	6.3	6.9	5.4	5.2
Asp27	4.0	2.6	1.1	0.9	Asp116	4.0	3.6	3.5	3.2
Lys32	10.4	9.1	10.9	10.8	Glu118	4.4	4.6	4.7	4.6
Arg33	12.0	13.1	12.9	13.4	Glu120	4.4	4.4[a]	4.5	4.4
Asp37	4.0	3.6	3.8	3.9	Asp122	4.0	3.1[a]	3.0	3.5
Lys38	10.4	13.3	14.5	13.4	HisA124	6.3	7.0	6.6	7.0
Arg44	12.0	12.7	11.9	11.7	Asp127	4.0	2.8[a]	3.1	3.0
HisA45	6.3	5.2	5.7	6.8	Tyr128	9.6	12.0	11.7	11.5
Glu48	4.4	3.7	3.8	3.7	Glu129	4.4	5.0	5.8[a]	4.8[a]
Arg52	12.0	12.4	13.6	13.6	Asp131	4.0	4.0	3.8[a]	3.7[a]
Arg57	12.0	12.4	15.1	15.1	Asp132	4.0	4.2	4.8	4.6
Lys58	10.4	10.8	11.0	11.2	Glu134	4.4	5.1	4.5	4.5
Asp69	4.0	2.3	2.6	2.0	Glu139	4.4	3.2	3.5	3.1
Asp70	4.0	3.8	3.9	4.1	HisA141	6.3	7.7	7.3	7.7
Arg71	12.0	12.7	13.0	12.8	Asp142	4.0	4.0	3.9	4.1
Lys76	10.4	10.6	10.6	10.6[a]	Asp144	4.0	3.1	2.8	3.3
Asp79	4.0	3.0	3.4	3.5	HisA149	6.3	6.7	6.7	6.7
Glu80	4.4	3.6	3.5	3.7	Tyr151	9.6	11.8	12.3	12.1
Asp87	4.0	3.9	3.8	1.8	Glu154	4.4	4.3	11.2	11.2
Glu90	4.4	1.8	1.3	1.8	Glu157	4.4	4.6	4.4	4.7
Arg98	12.0	12.1	12.3	12.8	Arg158	12.0	14.0	14.3	14.1
Tyr100	9.6	11.5	12.8	12.2	ArgC159	12.0	13.7	13.9	13.6[a]
Glu101	4.4	3.7	3.3	3.3	ArgC159	3.8	3.6	3.7	3.5

[a] Residue incomplete in crystal structure and was built using the Quanta/CHARMm molecular editor.

References

Cannon, W. R., Garrison, B. J. & Benkovic, S. J. (1997). Electrostatic characterization of enzyme complexes: reevaluation of the mechanism of catalysis of dihydrofolate reductase. *J. Am. Chem. Soc.***119**, 2386–2395.

Edited by B. Honig

(Received 4 April 1997; received in revised form 21 May 1997; accepted 21 May 1997)